

Optimisation of the Current Profile with far off-axis ECH Power

Deposition in high Elongation TCV Plasmas

A. Pochelon, Y. Camenen, F. Hofmann, S. Alberti, C. Angioni, T.P. Goodman,
M.A. Henderson, P. Nikkola, L. Porte, O. Sauter, A. Scarabosio

*Centre de Recherche en Physique des Plasmas
Association EURATOM-Confédération Suisse
Ecole Polytechnique Fédérale de Lausanne
1015 Lausanne, Switzerland*

Introduction: Plasma shaping is a means to improve tokamak performance. In order to test the β -limit predicted by ideal MHD for highly elongated plasmas, one has to achieve discharges at a normalised plasma current $I_N = I_p / aB \sim 2 \text{ MA/mT}$. Highly elongated discharges are, however, vertically unstable and can only be stabilised by providing sufficient current density close to the plasma edge. In ohmic discharges, this is achieved operating at a low safety factor q_{edge} . In TCV, ohmic plasmas with an elongation $2.2 < \kappa < 2.8$ have been stabilised at high $I_N \sim 2.8$ - 3.5 MA/mT [1]. In order to extend the range of equilibria to lower I_N , where ohmic discharges are no longer stable, current profile broadening by a non-ohmic method is required. Far off-axis 2nd harmonic X-mode ECH (X2) has been applied in TCV [2,3] allowing the creation of highly elongated discharges ($\kappa \sim 2.48$) at low current and high safety factor ($I_N \sim 1.05 \text{ MA/mT}$, $q_{\text{edge}} \sim 10$). Increasing the current towards $I_N \sim 2$ requires more X2 power to broaden the current profile, stressing the needs of optimising the efficiency of this method. This paper presents parametric dependencies of far off-axis ECH current profile broadening and initial tests of 3rd harmonic central heating to increase the plasma β .

ECH system: TCV is capable of delivering 4.5MW ECH power for 2s pulse length: 3MW at the 2nd harmonic and 1.5MW at the 3rd harmonic (X3). The X2 system is composed of six 500kW gyrotrons at 82.7GHz with six independent low field side (LFS) launchers (four upper lateral and two equatorial), steerable during the discharge. The X3 system is composed of three 500kW gyrotrons at 118GHz with one independent top launcher, also steerable during the discharge. The cut-off density of X2 and X3 waves is respectively 4.25 and $11.5 \cdot 10^{19} \text{ m}^{-3}$.

ECH high elongation experiments: Typical time traces are shown in **Fig. 1**. Just before ECH turn on in the ohmic phase, the target plasma has an intermediate elongation ($\kappa \sim 1.75$) and the pre-programmed quadrupole and hexapole fields are then kept constant throughout the ohmic and the EC heated phase. X2 power is deposited far off-axis ($\rho_{\text{dep}} = (V_{\text{dep}} / V_{\text{max}})^{1/2} > 0.5$), using upper lateral launchers because their shorter beam path reduces refraction effects at high density. The local EC power deposition leads to a local increase of the temperature, which modifies the resistivity profile. The inductive current profile is consequently broadened and the plasma elongation κ increases. The κ ramp-up duration gives the order of magnitude of the current diffusion time.

Current profile analysis: Since the quadrupole and hexapole fields are kept constant during the discharge, a *plasma elongation* increase is necessarily due to a broadening of the current profile. The modification of the current profile is essentially due to the modification of the resistivity profile (ECCD and bootstrap current represent $\sim 8\%$ of the total plasma current), so that the *temperature profile* is also an indicator of the current profile in the asymptotic limit. The *internal inductance* l_i is computed by the equilibrium reconstruction code LIUQE using

magnetic measurements [4]. It decreases when the elongation increases or when the current profile is broadened. For instance, if κ is increased from 1.75 to 2.4 without any change of the current profile, l_i decreases by 8%. To separate the direct plasma shape influence, we can define a normalised inductance $l_i^* \sim l_i (I^2/4\pi S)$, where S is the plasma cross section area, and l a parameter depending on the plasma cross section perimeter and on the poloidal magnetic field [5]. The proportionality constant is chosen to have $l_i^* = l_i$ at the beginning of the EC heating for a standard shot. We define Δl_i^* as the difference between l_i^* at the start of EC heating and the asymptotic value during the plateau period. The ECH deposition location and the plasma first-pass power absorption are computed with the ray tracing code TORAY-GA [6]. The experimental results are compared to the fixed boundary transport code PRETOR based on the RLW model [7,8].

Deposition location and power dependence: The standard parameters are $I_p \sim 300\text{kA}$, $n_{e0} \sim 2.5 \cdot 10^{19}\text{m}^{-3}$ (to avoid strong refraction), $P_{EC} \sim 1\text{MW}$, $\rho_{dep} \sim 0.7$, fixed launchers with the same ρ_{dep} ($\Delta\rho=0$), no toroidal angle ($\varphi=0$). The explored parameter range is $0 < P_{EC} < 1.8\text{MW}$ and $0.1 < \rho_{dep} < 0.8$ [5].

The influence of the deposition location on the current profile is shown in **Fig. 2**. The optimal EC power deposition location for broadening the current profile appears to be a rather narrow region, $0.55 < \rho_{dep} < 0.7$, both from experiment and transport simulation. With a deposition inside $\rho \sim 0.55$, the current profile broadening effect is reduced and becomes even inverted for $\rho_{dep} < 0.4$ (current profile peaking for the experiment and the PRETOR simulation). On the other hand, for $\rho_{dep} > 0.75$, the deposited EC power is not well confined and the action on the current profile is reduced. The values of the internal inductance computed by LIUQE and the one computed by PRETOR are slightly different, which can be explained by the choice of the current profile functional in the LIUQE reconstruction, optimised for ohmic profiles.

The effect of the EC power launched is shown in **Fig 3**. More than 90% of the power launched is absorbed at the first pass. The current profile broadening effect increases first steeply with the total absorbed power before saturating above $P_{abs} \sim 0.45\text{MW}$. The saturation is very pronounced on the total internal inductance variation Δl_i^* and is partly explained by the ρ_{dep} asymptotic value: for $P_{abs} > 0.45\text{MW}$, the asymptotic ρ_{dep} reaches the low value of $\rho_{dep} \sim 0.51$, where the scheme loses in efficiency, according to the result of **Fig. 2**. The saturation is less pronounced but still visible on the initial $-l_i^*$ ramp rate (not shown here) or for the PRETOR simulation, which are both obtained at constant, optimal ρ_{dep} .

The saturation with power found at constant ρ_{dep} both on the initial l_i^* ramp rate and in the PRETOR simulations suggests a non-linear increase thermal diffusivity χ_e with absorbed power. The χ_e profiles corresponding to the data of **Fig. 3** are shown in **Fig. 4**. χ_e is shown to increase with power just outside the deposition radius, corresponding to a global electron confinement time τ_{Ee} decrease of 6.5 to 3.5ms.

Overdense operation: In the search of optimising the efficiency of off-axis deposition to increase plasma elongation, operating at high density has been found to allow the highest elongations with the lowest X2 power for a given plasma current. The increase of elongation with density at constant injected power is shown in **Fig. 5a**. It has been regularly observed in the ohmic elongation experiments in TCV that l_i decreases with density. This is further observed with off-axis ECH and can be inferred from the electron temperature profile: in **Fig.**

5b, the $T_e^{3/2}$ profile is shown to be flattened on axis at high density, which results in a broadening of the current profile.

With off-axis heating at low current, 300kA, sawteeth are lost during the elongation ramp-up when q_0 moves above unity, without noticeable mode activity. At high density, a burst of internal modes occurs at the $q_0 \sim 1$ crossing. At higher density, this mode activity persists during the full discharge. The mode activity is analysed with the help of the 64 channel multiwire proportional soft X-ray diagnostic [9], and reveals an $m=1, 2, 3$ mode structure inside the inversion radius, **Fig. 6**. The very flat spectrum measured, where the $m=2$ and 3 mode amplitude are respectively 70% and 20% of the $m=1$ amplitude, is a typical signature of a flat current profile [10].

Initial experiments with central X3 deposition: The use of far off-axis X2 ECH in high density discharges has allowed increasing substantially the range of elongated equilibria at intermediate currents, as shown in **Fig. 7**. High density equilibria, that are overdense in the core, provide interesting target plasmas for X3 heating. An example of an initial experiment of X3 central power deposition [11] is shown in **Fig. 8**. The plasma has an elongation of 2.36 and is centrally overdense to X2. The Thomson electron temperature is increased by 1keV with 0.5MW of X3 heating, reaching $\beta_T \sim 1\%$. The drop in κ and the increase in l_i is partly due to the central heating, which peaks the current profile on a typical current diffusion time scale, making the mode activity of Fig. 6 disappear in some 20ms.

Conclusions: With the help of far off-axis X2 power deposition used to broaden the current profile and to elongate the plasma, high elongation high density discharges at intermediate I_N have been created to study their confinement properties with X3 central heating.

This work was partially supported by the Swiss National Science Foundation.

References

- [1] F. Hofmann, et al., Phys. Rev. Lett. **81**, (1998) 2918.
- [2] A. Pochelon, et al., Nucl. Fusion **41** (2001) 1663.
- [3] F. Hofmann, et al., Plasma Physics and Controlled Fusion, **43** (2001) A161.
- [4] F. Hofmann, et al., EPS Conf. on Plasma Phys. and Contt. Fus., Vol. **19**, Part II (1995) 100.
- [5] Y. Camenen et al., Proc. of EC-12, Aix-en-Provence, France, May 2002.
- [6] K. Matsuda, IEEE Trans. Plasma Sci. **17** (1989) 6.
- [7] D. Boucher et al., IAEA TCM Adv. in Simul. & Model. Thermonucl. Plasmas, Montreal (1993)142.
- [8] C. Angioni, et al., Theory of Fus. Plasmas, Varenna 2000, ISSP-19 (Ed. Comp, Bologna, 2001) 73.
- [9] A. Sushkov et al., this conference, P4.118.
- [10] P-A. Duperrex et al., Nucl. Fusion **32** (1992) 1161.
- [11] S. Alberti et al., this conference, P2.073.

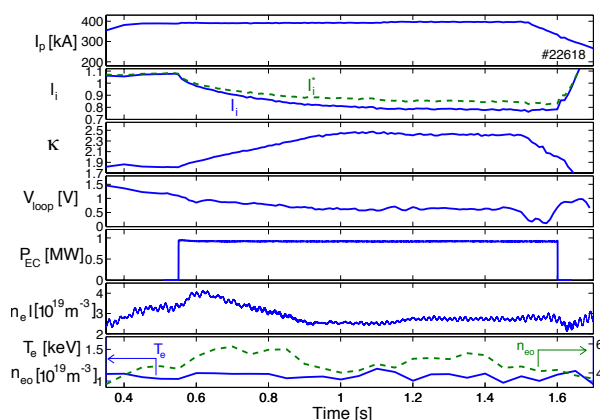


Fig. 1 Decrease of I_i and increase of κ with far off-axis ECH applied in the current plateau.

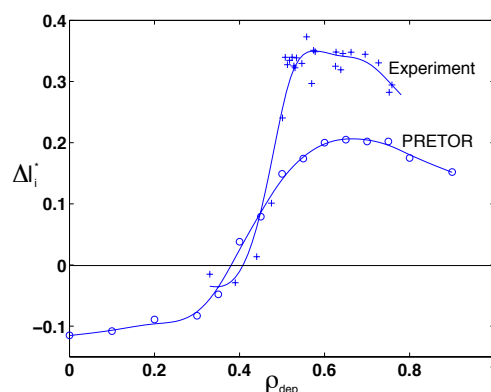


Fig. 2 Current profile change for different radial deposition location ρ_{dep} . $I_p=300kA$, $P_{EC}=1MW$.

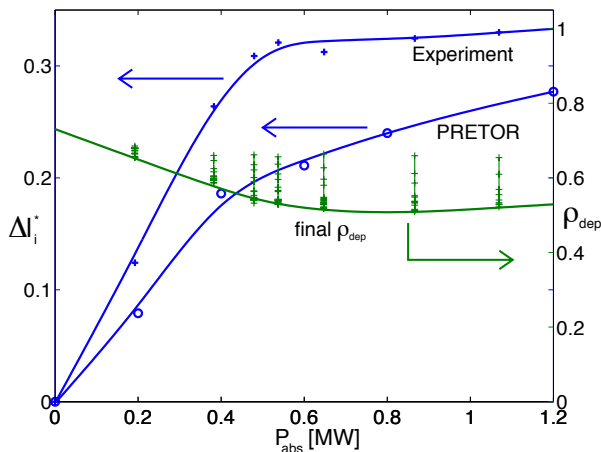


Fig. 3 Current profile change for different absorbed power, from experiment and from PRETOR. $\rho_{dep}=0.7$, $I_p=300kA$, $n_{eo}\sim 2.5 \cdot 10^{19} m^{-3}$.

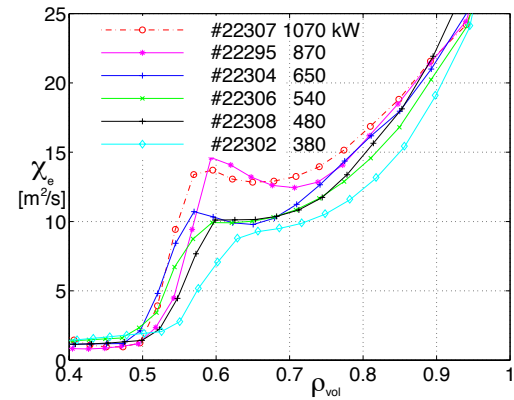


Fig. 4 Current diffusivity χ_e for the power scan of fig. 3.

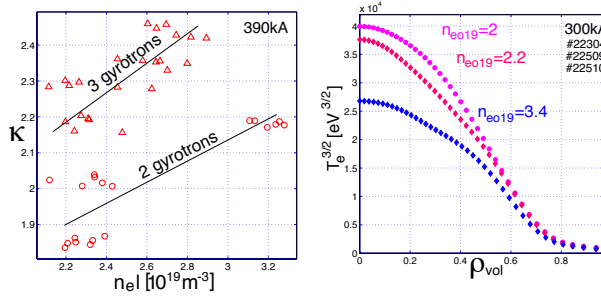


Fig. 5a, b High density operation: a) κ improves with density at constant EC power, b) the resistivity deduced current profile is flattened and therefore broadened with density.

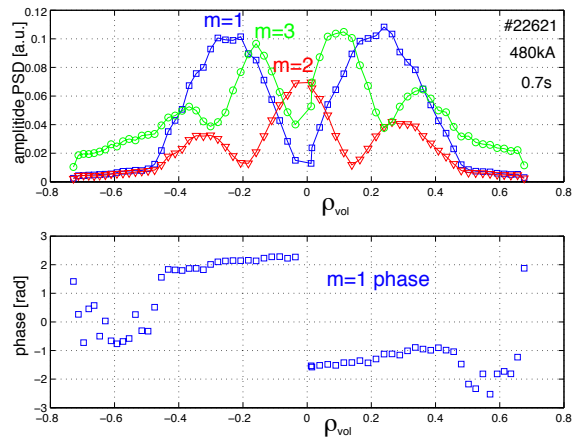


Fig. 6 $m=1,2,3$ mode activity inside inversion radius $\rho_{inv}=0.4$, from the 64 channel soft X-ray multiwire proportional chamber diagnostic.

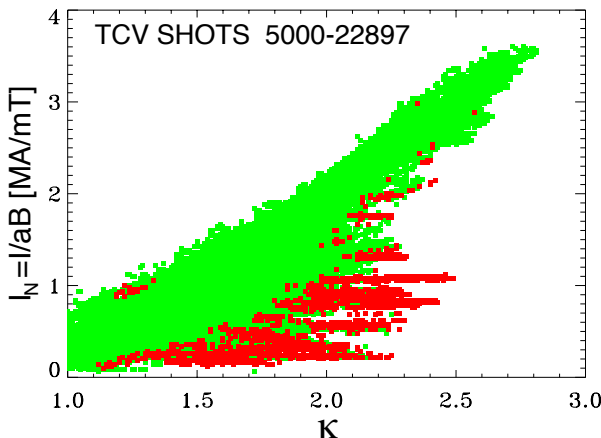


Fig. 7 Range of TCV operation in TCV: Ohmic discharges (green) and ECH (red). Off-axis ECH allowed reaching $\kappa=2.48$ at low I_N .

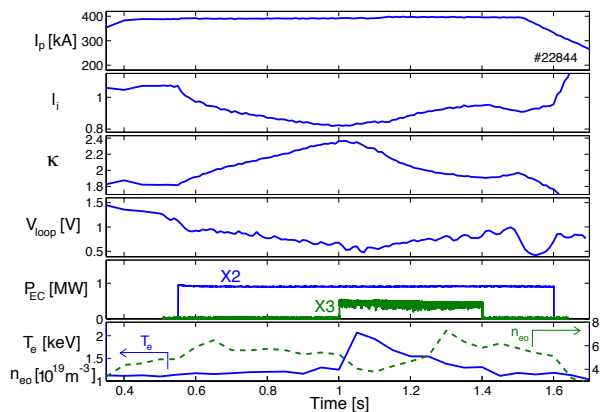


Fig. 8 X3 central heating (0.5MW) on a high density high elongation off-axis heated prepared target.